ON THE RELATION BETWEEN INDENTATION HARDNESS AND THE TRUE STRESS-STRAIN CONSTITUTIVE BEHAVIOR OF A MATERIAL—G. R. Odette, M. Y. He, and D. Klingensmith (University of California, Santa Barbara)

OBJECTIVE

Our objective is to develop a rigorous general relation between indentation hardness (H) and the true stress-strain constitutive $\sigma(\varepsilon)$ laws governing the plastic deformation of metals and alloys.

SUMMARY

A new and powerful indentation hardness (H) approach to evaluating the true stress (σ)-true plastic strain (ε), $\sigma(\varepsilon)$, constitutive behavior of materials is described. Since measurements of H intrinsically probe a wide-range of ε (up to ≈0.5), accurate assessment of the corresponding yield (σ_y) stress and strain hardening [$\sigma_{sh}(\varepsilon)$] pose a significant challenge. Extensive elastic-plastic finite element (FE) simulations have been carried out to assess the relation between H and $\sigma(\varepsilon)$. The simulations were based on both a wide variety of analytical $\sigma(\varepsilon)$ relations, in the form of $\sigma(\varepsilon) = \sigma_y + \sigma_{sh}(\varepsilon)$, as well as actual $\sigma(\varepsilon)$ derived from data on a large number of alloys with a very wide range of constitutive behavior. The analysis led to derivation of a remarkable *universal relation* between H and $\sigma(\varepsilon)$ given by $H \approx 4.05(1 + 34.6\sigma_{flow}/E)\sigma_{flow}$, where $\sigma_{flow} = \sigma_y + \langle\sigma_{sh}\rangle$, $\langle\sigma_{sh}\rangle$ is the average strain hardening between ε = 0 and 10%, and E is the elastic modulus. Note we use consistent MKS units of MPa for both H and σ_{flow}. The expression for $H(\sigma_{flow})$ also can be inverted to one describing $\sigma_{flow}(H)$. Experimental σ_{flow}- H data pairs based on this definition of σ_{flow} for the large set of alloys noted above with a very diverse range of $\sigma(\varepsilon)$ are in excellent agreement with the model predictions. The σ_{flow}- H relation provides insight into the large variation of the H/σ_y ratios that are observed for different materials, as well as the corresponding variation in the $\Delta H/\Delta\sigma_y$ ratios used to estimate $\Delta\sigma_y$ due to irradiation based on measurements of ΔH. Applications of the H/σ_{flow} relation, including both evaluating $\langle\sigma_{sh}\rangle$ in materials that have very low uniform strain capacity in standard tensile tests and measuring at $\sigma(\varepsilon)$ high ε.

PROGRESS AND STATUS

Introduction

Microhardness (H) measurements provide a convenient, non-destructive means to evaluate the strength of materials, as well as to characterize effects such as irradiation hardening. However the relation of H to more quantitative measures of true stress-strain $\sigma(\varepsilon)$ constitutive properties, such as the yield stress (σ_y) and post-yield strain hardening (σ_{sh}), have remained ambiguous, and to a large extent semi-empirical. This is in large part due to the fact that H intrinsically probes a wide range of ε, hence, represents some average measure of an effective flow stress, $\sigma_{flow} = \sigma_y + \sigma_{sh}$. In principle, the decomposition of into σ_y and σ_{sh}, which is an appropriate physical form as proposed by Kocks and Mecking, as well as Zerrelli and Armstrong and others, provides a basis to better quantify the H-$\sigma(\varepsilon)$ relation. For a specified geometry, from a continuum perspective the H-$\sigma(\varepsilon)$ relation can depend only on σ_y, σ_{sh} averaged over some undefined and perhaps variable ε-range, E (or the indenter and material modulus) and the friction coefficient, μ. For example, in the case of a perfectly plastic material, the H/σ_y ratio would be expected to depend only weakly on E and μ. Further, while indentations produce a large range of ε (≈0 to 50%), they are finite and very small regions of high ε would be expected to have little effect on σ_{sh}. Thus we carried out and extensive series of finite element (FE) simulations of the relation between H and σ_y plus $\sigma_{sh}(\varepsilon)$ averaged over different strain ranges for a very wide range of $\sigma(\varepsilon)$ to assess the possibility of obtaining a of a universal master H-$\sigma(\varepsilon)$ relation.

We found such a relation in the form $H = 4.05(1 + 34.6\sigma_{flow}/E)\sigma_{flow}$, where $\sigma_{flow} = \sigma_y + \langle\sigma_{sh}\rangle$, $\langle\sigma_{sh}\rangle$ is the average strain hardening between ε = 0 and 10% and E is the elastic modulus. We show that the master relation provides insight into the large variation of the H/σ_y ratios that are observed for different materials, as well as the corresponding variation in the $\Delta H/\Delta\sigma_y$ ratios used to assess effects such as hardening due

to irradiation. We also show that useful applications of the H/σ_{flow} relation are to evaluate $<\sigma_{sh}>$ in materials that have very low uniform strain capacity in standard tensile tests as well as to measure $\sigma(\varepsilon)$ high ε.

Finite Element Modeling of Indentation Harness (H)

Cone indentations were simulated using the general purpose FE code ABAQUS. The plasticity model in ABAQUS is based on J_2-incremental flow theory. The inputs to ABAQUS are E, σ_y, $\sigma_{sh}(\varepsilon)$ and the contact interface friction coefficient (μ). The cone indenter, with an angle of 68.2^o, was treated as two-dimensional (z, r, symmetric in θ) rigid body. The two-dimensional half space mesh had 3021 four-node quadrilateral axisymmetric elements with 3232 nodes. The radial (R) and depth (z) dimensions of the mesh were ≈ $50D_{max}$ and $20D_{max}$, respectively, where D_{max} is the maximum penetration depth of the cone. The mesh was refined in the area under the indenter (Fig. 1) and there were more than 20 elements in the contact area under the indenter at maximum load. The calculations were carried out for a prescribed loading/unloading cycle to a maximum load P. Hardness, H, was calculated as P/A, where A is the area of the permanent indentation, $\pi D^2/4$, where D is the diameter of the indentation at the plane of the undeformed specimen surface. Test calculations were carried out to demonstrate that H was independent of the mesh size and a convergence study showed that the meshes provided accurate results for displacements and the pile-up shape.

The friction between the specimen and the indenter affects the shape of the pile-up. For μ <0.2, the effects of μ are significant. However, the pile-up shape is insensitive to μ ≥0.2. Since the nominal μ for such contacts is ≈0.2 to 0.3, μ = 0.2 was used in the FE simulations. The calculated H values are also insensitive to the load P between 40 and 200g. The effective plastic strain reached 0.5 directly underneath the indenter, so this was used as an upper bound for the strain range (Fig. 2).

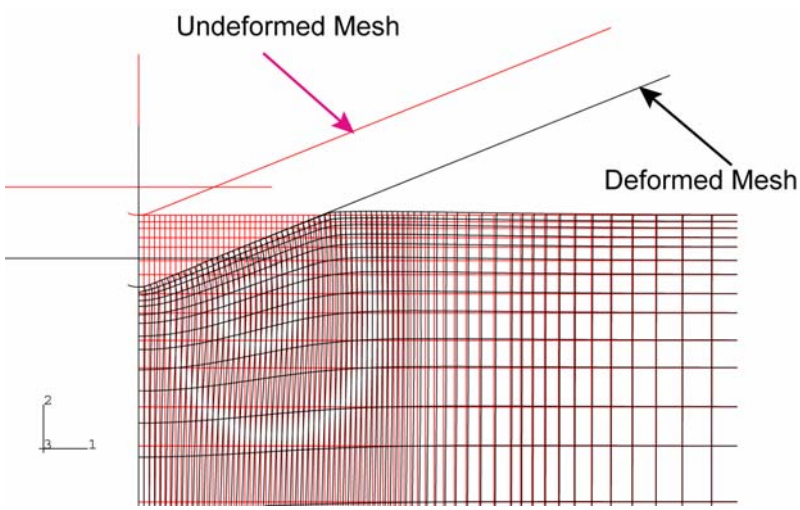

Fig. 1. Section of the mesh used in the FE simulations of H.

One large set of simulations were carried out for E = 200 GPa and constitutive laws in the form:

$$\sigma(\varepsilon) = \sigma_y \qquad \varepsilon \le \varepsilon_y \qquad (1a)$$

$$\sigma(\varepsilon) = \sigma_y + \sigma_{sh} = \sigma_y + \sigma_{shm}[1-\exp(-\gamma(\varepsilon-\varepsilon_y)] \qquad \varepsilon > \varepsilon_y \qquad (1b)$$

The H were calculated for a Luder's-yield strain (ε_y = 0.005) and a wide range of σ_y (100–850), maximum saturated strain hardening levels (σ_{shm} = 125–500) and pre-saturation hardening rates (γ = 3 to 15) (Fig. 3). The calculations were also carried out for actual $\sigma_{sh}(\varepsilon)$ curves derived from tensile tests on a large number of alloys with a very diverse range of constitutive properties ranging from annealed stainless

steels with low σ_y and γ and high σ_{shm}, to martensitic steels with intermediate σ_y and σ_{shm} and high γ, to TiNb with very low σ_{shm}. The materials also included unirradiated and irradiated Mn-Mo reactor pressure vessel (RPV) steels, as well as alloys with large Luders strain regions up to ε_l ≈10% and pre-strained materials.

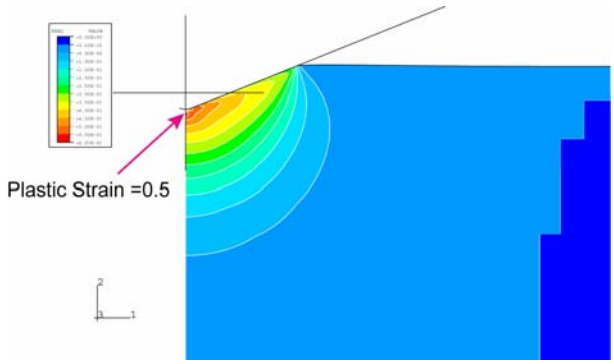

Fig. 2. A typical example of the effective strain distribution under the indenter.

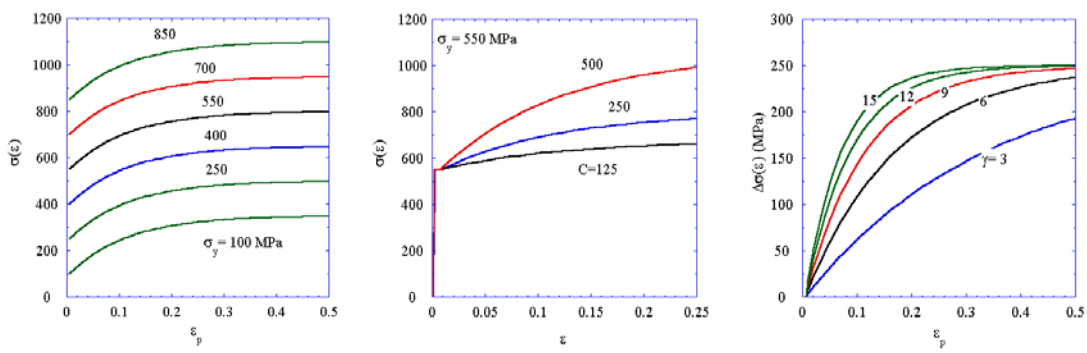

Fig. 3. Analytical σ(ε) laws used in the FE simulations of H.

Results

The σ_y versus H for σ_{shm} =0, 250, and 500 MPa and γ = 9 are shown in Fig. 4. The σ_y increases with H as $\sigma_y \approx A + 0.3H$, with A ≈25, 100 and 170 MPa for σ_{shm} = 0, 250, and 500 MPa, respectively. The corresponding positive offsets on the H axis primarily reflect a contribution to H of the $\sigma_{sh}(\varepsilon)$ averaged over some effective increment of effective plastic strain, ε, under the indent. In other words the σ_{flow} probed by H is larger than σ_y by an effective ε-averaged $<\sigma_{sh}>$.

Thus the FE H data for the various $\sigma(\varepsilon)$ were analyzed by calculating the $<\sigma_{sh}>$ between various lower (ε_l) and upper (ε_u) limits and fitting the corresponding $\sigma_{flow} = \sigma_y + <\sigma_{sh}>$ versus H data with a function in the form:

$$H = C_1(1 + C_2\sigma_{flow})\sigma_{flow} \qquad (2)$$

Here C_1 and C_2 are weak functions of ε_l and ε_u. An optimum set of ε_u and ε_l can be determined by minimizing the standard deviation (δH) of the fit for the predicted H_p from Equation 2 to the FE simulations H_c as a function of ε_l and ε_u as:

$$\delta H = [\Sigma_j(H_{pn} - H_m)^2]^{1/2} \qquad (3)$$

for all values of H for the j different $\sigma(\varepsilon)$. We found that values of $\varepsilon_l \approx 0.0$ and $\varepsilon_u \approx 10\%$ gives a very good fit as shown by the solid line in Fig. 5 given by:

$$H=4.05(1 - 0.000173\sigma_{flow})\sigma_{flow} \quad (4)$$

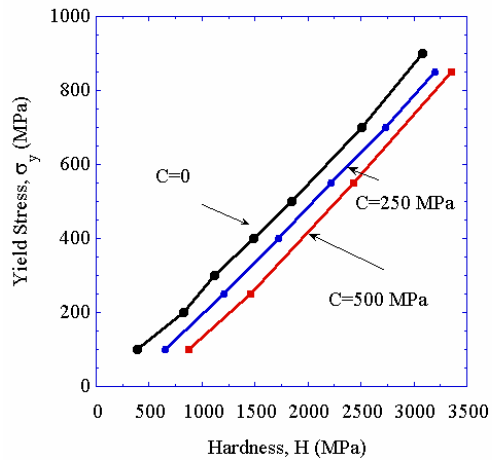

Fig. 4. The σ_y versus the FE simulations of H for different σ_{shm} (= C).

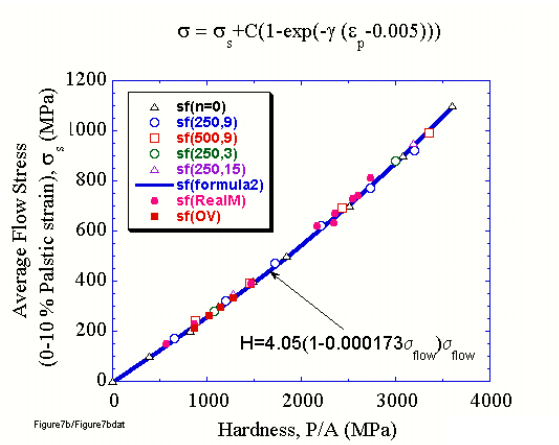

Fig. 5. The $\sigma_{flow} = \sigma_y + \langle\sigma_{sh}\rangle$ versus H for a wide range of $\sigma(\varepsilon)$.

These results are all for E = 200GPa. Thus the curvature in the σ_{flow} versus H relation is likely due to the corresponding variation in σ_{flow}/E. The H/σ_{flow} ratio would be expected to decrease with increasing σ_{flow}/E due to effects such as the constraint on the region of plastic deformation and reverse plasticity. Figure 6 shows the H/σ_{flow} for versus σ_{flow}/E, including additional calculations for E = 50, 100, and 400 GPa for the same $\sigma(\varepsilon)$. As expected, the variation in H/σ_{flow} in the initial calculations is consistent with variations in σ_{flow}/E. Thus Equation 4 can be rewritten as:

$$H=4.05(1 - 34.6\sigma_{flow}/E)\sigma_{flow} \quad (5)$$

However, the results in Fig. 6 show that the linear relation breaks down at $\sigma_{flow}/E > 0.006$. A second order polynomial fit to the σ_{flow}/H for versus σ_{flow}/E data yields:

$$H=4.08(1 + 1755[\sigma_{flow}/E]^2 - 44.1[\sigma_{flow}/E])\sigma_{flow} \qquad (6)$$

Additional calculations will be needed between $\sigma_{flow}/E = 0.006$ and 0.012 to confirm the non-linear fit. However, for most materials of interest, $\sigma_{flow}/E < 0.006$; hence, Equation 4 gives an adequate representation of the FE results.

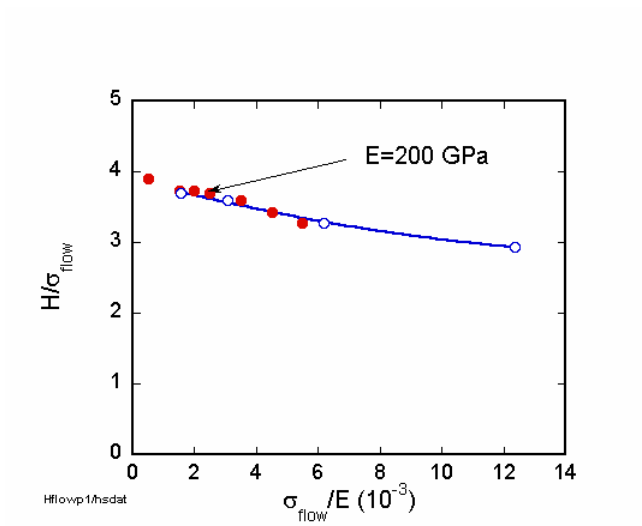

Fig. 6. The σ_{flow}/H versus σ_{flow}/E.

Comparison with Experiment

As noted above, tensile tests were conducted on a large number of materials with a very diverse range of $\sigma(\varepsilon)$. Vickers diamond pyramid hardness (DPH) measurements were also made on these same materials in order to evaluate the FE predictions. The $\sigma_{flow} = \sigma_y + \langle\sigma_{sh}\rangle$ were directly assessed based on the experimental $\sigma_{sh}(\varepsilon) = \sigma(\varepsilon) - \sigma_y$ converted from engineering stress strain curves up to the onset of necking and averaged between $\varepsilon = 0$ and 10%. Figure 7 compares the experimental σ_{flow} versus H data to the predictions of Equation 4. The agreement is generally very good, although the experimental data tends to fall slightly above the prediction line, especially at lower H; and overall the experimental σ_{flow} versus H relation is more linear than the FE results. FE simulations of diamond pyramid indenter hardness (DPH) show that H_{DPH} are only slightly larger than for cone in indentation, thus variations in the indenter geometry do not explain the modest differences between experimental data and FE predictions of σ_{flow}. We plan to evaluate the effect of a non-rigid indenter next to see if this makes a difference. However, considering the uncertainties in the data and simplicity of the model, we believe the agreement between experiment observations and the FE based universal σ_{flow} - H relation is excellent and provides strong support for use of Equations 4 or 5.

Discussion and Applications

The universal master σ_{flow} - H relation is remarkable in view of the much larger ε-range created by the indentation (see Fig. 3). However, it permits a quantitative understanding of a number of empirical trends, such as:

1. That there is a large variation in the observed H/σ_y ratios due to the effects of both $<\sigma_{sh}>$ and σ_{flow}/E.

2. That the ratio of H/σ_y tends to be higher for steels with low σ_y due to the effect of σ_{flow}/E.

3. That the $\Delta H/\Delta\sigma_y$ following irradiation is generally lower than the unirradiated H/σ_y with irradiation due to reduction in $<\sigma_{sh}>$.

In addition, the universal relation allows combining H and σ_y measurements from a tensile test to estimation of strain hardening in alloys with very low uniform tensile strain as:

$$<\sigma_{sh}> = \sigma_{flow}(\text{from H}) - \sigma_y(\text{from a tensile test})$$

The universal relation also permits a convenient method to evaluate $\sigma(\varepsilon)$ high ε regions by making H measurements on pre-strained materials. An effective way to do this is to make hardness transverses on sections of a bent beam that undergoes stable plastic deformation over a wide range of effective ε. Indeed, such transverses from regions of high deformation across the neutral axis not only assess regions with ≈0 to very high ε, but also involve complex and varying stress that yield information of plasticity flow laws and tensile to compressive deformation effects on $\sigma(\varepsilon)$j.

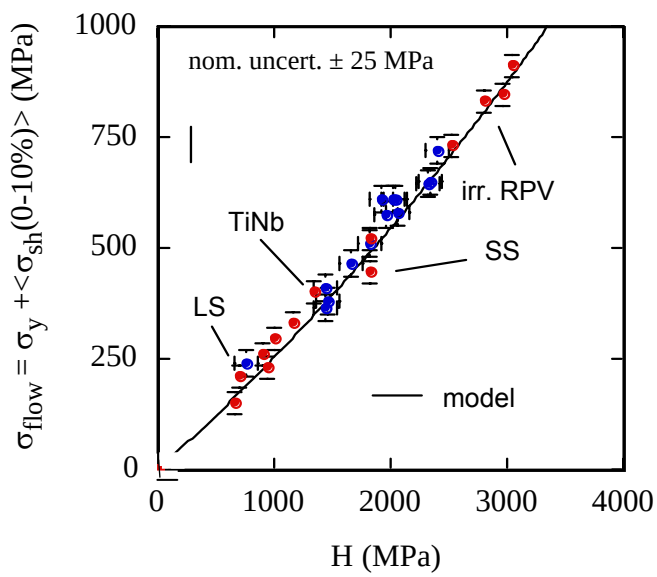

Fig. 7. Pairs of σ_{flow}-H data points for materials with a wide range of compared to the FE model prediction.

Future Research

Future research will focus on the following items:

1. Assessment of the effect of the elastic modulus of the indenter.

2. Additional experimental verification of the σ_{flow}-H relation with an even wider range of materials.

3. Application of the method to assessing $<\sigma_{sh}>$ in materials that undergo immediate necking.

4. Assessing the $\sigma(\varepsilon)$ at high ε in pre-deformed materials.

5. Evaluation of the effects of variations in stress state history on $<\sigma_{sh}>$.